Analysis of the Radial Stiffness of Rubber Bush Used in Dynamic Vibration Absorber Based on Artificial Neural Network

Lie Li, Beibei Sun*, Miao He, Haitao Hua

ABSTRACT

Rubber bush is used in dynamic vibration absorber as dissipating devices in damping boring bar. These devices actually have to support radial load in compression when chattering occurs. Mastering the behavior of the radial stiffness of the rubber bush implies an accurate understanding of dynamic vibration absorber. The behavior is, however, complex due to the changeable cross-sectional shape and boundary conditions of the rubber bush. By using artificial neural network, the radial stiffness can be predicted efficiently. According to the authors' knowledge, simulations and tests on radial stiffness of the rubber bush under combined different cross-sectional shape and boundary conditions by using artificial neural network have not been performed yet. The purpose of this study is thus to find the law of radial stiffness of rubber bush under different cross-section shapes and axial pre-compression conditions. In order to achieve this aim, simulations and tests under different chamfering sizes and axial pre-compression by using artificial neural network were first carried out.

Key Words: Artificial Neural Network, Dynamic Vibration Absorber, Rubber Bush, Radial Stiffness, Axial Pre-Compression

DOI Number: 10.14704/nq.2018.16.6.1643 **NeuroQuantology 2018; 16(6):737-744**

Introduction

Dynamic vibration absorbers are widely used in the vibration control of various products and have the characteristics of simple structure, convenient layout, and high reliability (Cui *et al*., 2018; Miguelez *et al.*, 2010; Zaoui *et al*., 2017). In recent years, with the improvement of NVH performance requirements for industrial products, dynamic vibration absorbers have been more and more widely used in the engineering industry (Cheng *et al*., 2017; Liu *et al*., 2017; Yang *et al.*, 2017). The background of this paper is the vibration control of the damping boring bar used for deep hole boring bar (Rubio *et al.*, 2013; Siddhpura and Paurobally, 2012; Quintana and Ciurana, 2011). In the deep hole boring, due to the large length to diameter ratio, the tool is prone to chatter. Placing a dynamic resonator inside the bar can play a good role in suppressing the vibration (Liu *et al.*, 2017). As shown in the Figure 1, the basic mechanism of the dynamic vibration absorber inside the bar consists of an inner and an outer sleeve, with a rubber bush between them.

The inner sleeve is fixed with the bar. When chattering occurs, the vibration energy is transmitted from the inner sleeve to the outer sleeve through the rubber bush. The chatter energy is dissipated through damping due to the vibration of the outer sleeve. It is easy to see that when chattering occurs, the radial stiffness of the rubber bushing plays a decisive role in the overall stiffness of the absorber. Therefore, the radial stiffness characteristics of the rubber bush have become the research focus of many

Corresponding author: Beibei Sun
Address: School of Mechanical Engineering, Southeast University, Nanjing 211189, China
e-mail ✉ bbsun@seu.edu.cn
Relevant conflicts of interest/financial disclosures: The authors declare that the research was conducted in the absence of any commercial or financial relationships that could be construed as a potential conflict of interest.
Received: 6 March 2018; **Accepted:** 27 April 2018

scholars. For a long time, people tried to give an accurate explanation of the constitutive features and eager to find analytical formulas that can describe the characteristics of rubber materials. However, due to the complex molecular properties, geometric shapes and boundary conditions, rubber exhibits strong multiple nonlinearity characteristics, which makes it difficult to establish mathematical models (Chuong *et al*., 2017). According to the knowledge of material mechanics and elastic mechanics, the stiffness formulas of some specific rubber materials can be obtained. However, when the shape is complex, it is difficult to obtain an accurate calculation formula (Maureira *et al.*, 2017; Markou and Manolis, 2018).

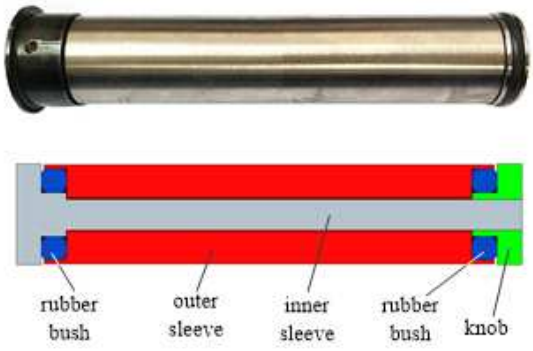

Figure1. Structure of the dynamic vibration absorber

A.C. Stevenson (1943) has focused on some boundary problems of two-dimensional elasticity; he focused on the setting up of boundary equations for problems of two-dimensional elasticity and obtained the dimensionless parameter calculation formula for radial stiffness. Adkins J E and Gent A N (1954) investigated the relation between applied force and deflection for bonded cylindrical rubber bush mountings of various dimensions theoretically and experimentally. For the symmetrical deformations of the elastic material, a theoretical treatment based on the classical linear theory of elasticity was found to predict the load of long and short bush length. Under conditions of plane strain and generalized plane stress respectively, the reduced radial stiffness, β_L and β_S, of long and short bushes were obtained, and the theoretical values of limiting stiffness were compared with the values measured experimentally. Horton (2000) derived the exact expression for the radial stiffness of a cylindrical rubber bush mounting of finite length, from which a convenient approximate representation was deduced. Some exact and approximate numerical results were compared with the experimental data obtained by Adkins and Gent . Then Horton and Tuphlme (2006) presented an extremely convenient closed-form approximation for the reduced radial stiffness of an annular rubber bush mounting of finite length. By using truncated Fourier and Fourier–Bessel series, Hill (1975) gave numerical values to the reduced radial stiffness, β, for a cylindrical bush of a finite length subjected to a radial load.

It is worth noting that there are some deficiencies in theoretical calculations:

(1) In terms of the cross-sectional shape, the rubber bush can only be a rectangular shaft section;

(2) In terms of the boundary conditions, the rubber bush can only be bonded to the rigid metallic inner and outer cylindrical sleeves;

(3) The boundary constraint of the rubber bush is difficult to be accurately described, and it is impossible to accurately describe the movement of the rubber bush during the loading process.

In order to find the law of the radial stiffness of the rubber bush under complex working conditions, Qin Bai (2008) built up the finite element model of annular rubber by using Ansys and achieved the fast and exact conversion between the radial stiffness and the parameters of annular rubber. Li Lie (2016) built the two-dimensional rigid flexible coupling model of the rubber bush; By using Abaqus/standard, the relationship between the radial stiffness and the axial compression were obtained. Although the finite element method can solve the problem of complex working conditions to some extent, it still needed to establish a solid model, which can help slove the problem of long modeling time and high computational cost. Artificial Neural network is a powerful tool for simulating non-deterministic system, which can be used to predict the radial stiffness of the rubber bush under complex conditions. Song (2017) estimated the upper limb muscle stiffness based on artificial neural network. Yuan (2006) presented stiffness function for all angular-contact ball bearings by a back-propagation neural network method. Although some scholars have used artificial neural networks for stiffness prediction, simulations and tests on radial stiffness of the rubber bush under combined different cross-sectional shape and boundary conditions by using artificial neural network have not been performed yet.

Establishment of neural network model

A feed-forward network with sigmoid hidden neurons and linear output neurons can fit multi-dimensional mapping problems arbitrarily well, given consistent data and enough neurons in its hidden layer. The network will be trained with Levenberg-Marquardt back-propagation algorithm, in which case scaled conjugate gradient back propagation will be used. It consists of a set of interrelated artificial neurons and uses a connectionist approach for calculations. A feed-forward network is an adaptive system modeling tool that can accurately reflect the operating status and characteristics of the system.

Back propagation (BP) neural network is a one-way communication network, consisting of input layer, hidden layer and output layer. There is a complete connection between the upper and lower layers, but there is no connection between the neurons in the same layer. The connection weights of each layers are changing and will be constantly adjusted during the learning process. When the training starts, the neural activation value is transmitted from the input layer to the output layer through the middle layer, and the output layer of the neural network can reflect the response corresponding to the input. If the desired target output cannot be obtained, the training will enter the back propagation stage and the output error will return to the input layer along the original connection path. By modifying the connection weights, the output error will gradually be reduced. Through continuous feedback, the accuracy of the output will be greatly improved. In the input layer, every node represents an input variable. The radial stiffness of the rubber bush is affected by its material, shape, and bonding surface (Ehsani *et al.*, 2015). In addition, the rubber bush has a certain amount of axial pre-compression during installation, which also has a significant influence on the radial stiffness. According to previous studies, in terms of materials, the radial stiffness of the rubber bush is mainly affected by the shear modulus, which is proportional to the radial stiffness. That is, for a specific material, the radial stiffness value of the rubber bush is determined once the shape is determined. Therefore, in this paper, material properties are no longer used as variables, and the effects of the shape of rubber ring and the axial pre-compression on radial stiffness are studied for a specific material. Thus the chamfering sizes and axial pre-compressions are chosen as the input variables.

Hidden layer design is the key part of the entire neural network, which is closely related to the prediction accuracy. Training accuracy can be improved by setting a reasonable number of nodes. The number of hidden nodes is determined by (Shuran and Shujin, 2011; Cheng *et al.*, 2013):

$$m = \sqrt{n+l} + \alpha \tag{1}$$

where n is the number of the input layer nodes, l is the number of output layer nodes, and α is an adjustment constant ranging from 1 to 10. In this study, the number of the hidden layer is set to be six by using trial and error method.

In the output layer, the radial stiffness is chosen as the output variable. Then a 2-6-1 BP neural network model is established as seen in Figure 2. The results can be obtained by (Yoon *et al.*, 2012):

$$\boldsymbol{y} = \boldsymbol{f}_2(\boldsymbol{w}_2 \boldsymbol{f}_1(\boldsymbol{w}_1 \boldsymbol{x} + \boldsymbol{b}_1)) + \boldsymbol{b}_2 \tag{2}$$

where y is the output variables, w is the weight, b is the bias, x is the input variables, f_1 is the tan-sigmoid function of "logsig", and f_2 is the linear function of "purelin".

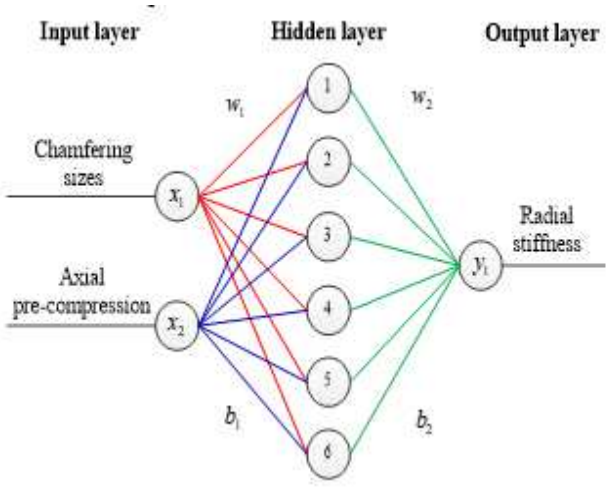

Figure 2. Structure of BP neural network model

Data collection

In order to obtain a good training effect, a large number of training samples are needed. However, if all the training samples are obtained from experiments, it will cost a long time. Therefore, only some specific samples such as the radial stiffness values of different chamferings and different axial compressions are obtained through experiments. Then, the finite element model is

established by using Abaqus, and the finite element model parameters are adjusted to verify the correctness of the finite element model. Finally, samples can be obtained through a large number of finite element simulations.

Experiments

Experiments under different chamfering sizes and axial pre-compressions are carried out to confirm the law of radial stiffness of rubber bush. Figure 3 shows the specific rubber bush samples with different chamfering sizes.

Figure 3. Rubber bushing samples with different chamfering sizes

The material properties of the rubber material can be obtained by testing the axial stiffness of the rubber. The axial stiffness is k_a=120N/mm

$$k_a = E_a \frac{\pi(D^2 - d^2)}{4h} \quad (3)$$

where D, d and h are the outside and inside diameter of the rubber bush. E_a is an appropriate apparent (or effective) Young's modulus. For rubber spring under pressure, the appropriate apparent Young's modulus is affected not only by the rubber material, but also by its shape and size, and generally satisfies: $E_a=iG$

where i is the geometric shape influencing factor. For an annular rubber bush, $i=3.6(1+1.65S^2)$, S is the ratio of the loaded bonded area to the force-free lateral surface area, $S = \frac{D-d}{4h}$. In this study, D=24.2mm, d=11.5mm, h=7.1mm, then G=0.5Mpa, E=1.5MPa. The material parameters can be seen in Table 1.

The tests are carried out on the pressure test platform as seen in Figure 4. The axial pre-compressions can be adjusted through the knob at the end of the dynamic vibration absorber. The force is plotted against different axial pre-compressions in Figure 5, and the legends 1, 2, 3, 4, 5 represent the intervals of the axial pre-compressions shown in the third column in Table 2. Since the maximum compression in working condition 1 is only 0.03 mm, only three intervals are selected for study. In other conditions, the maximum compression is divided into five equal intervals.

Table 1. Material parameters of the rubber bushing samples

Material	H_s	E(MPa)	G(MPa)
Natural rubber	40	1.5	0.5

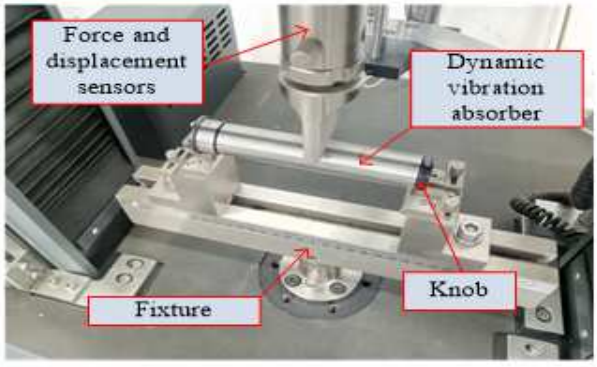

Figure 4. Test of radial stiffness under different axial pre-compressions

It is easy to find that the force-displacement is almost a straight line because in the case of small deformation and small load, the radial stiffness is stable. By deriving, the apparent radial stiffness K_{appt} can be easily obtained. As there are two rubber bushes placed parallel in a dynamic vibration absorber, the radial stiffness of each rubber bush can be calculated as:

$$K_{expt} = \frac{K_{appt}}{2} \quad (4)$$

Table 2. Measured radial stiffness

No.	R(mm)	Axial pre-compressions s(mm)	K_{expt}(N/mm)
1	0.5	0.01, 0.02, 0.03	69.23, 77.50, 105.61
2	1	0.026, 0.052, 0.078, 0.104, 0.13	55.23, 122.84, 201.86, 299.65, 412.62
3	1.5	0.06, 0.12, 0.18, 0.24, 0.30	162.23, 213.29, 282.5, 374.41, 498.28
4	2	0.108, 0.216, 0.312, 0.432, 0.540	76.63, 115.66, 164.45, 229.64, 309.99
5	2.5	0.168, 0.336, 0.504, 0.672, 0.840	55.32, 78.26, 124.85, 195.36, 289.98
6	3	0.24, 0.48, 0.72, 0.96, 1.20	32.56, 61.54, 88.22, 144.36, 224.56

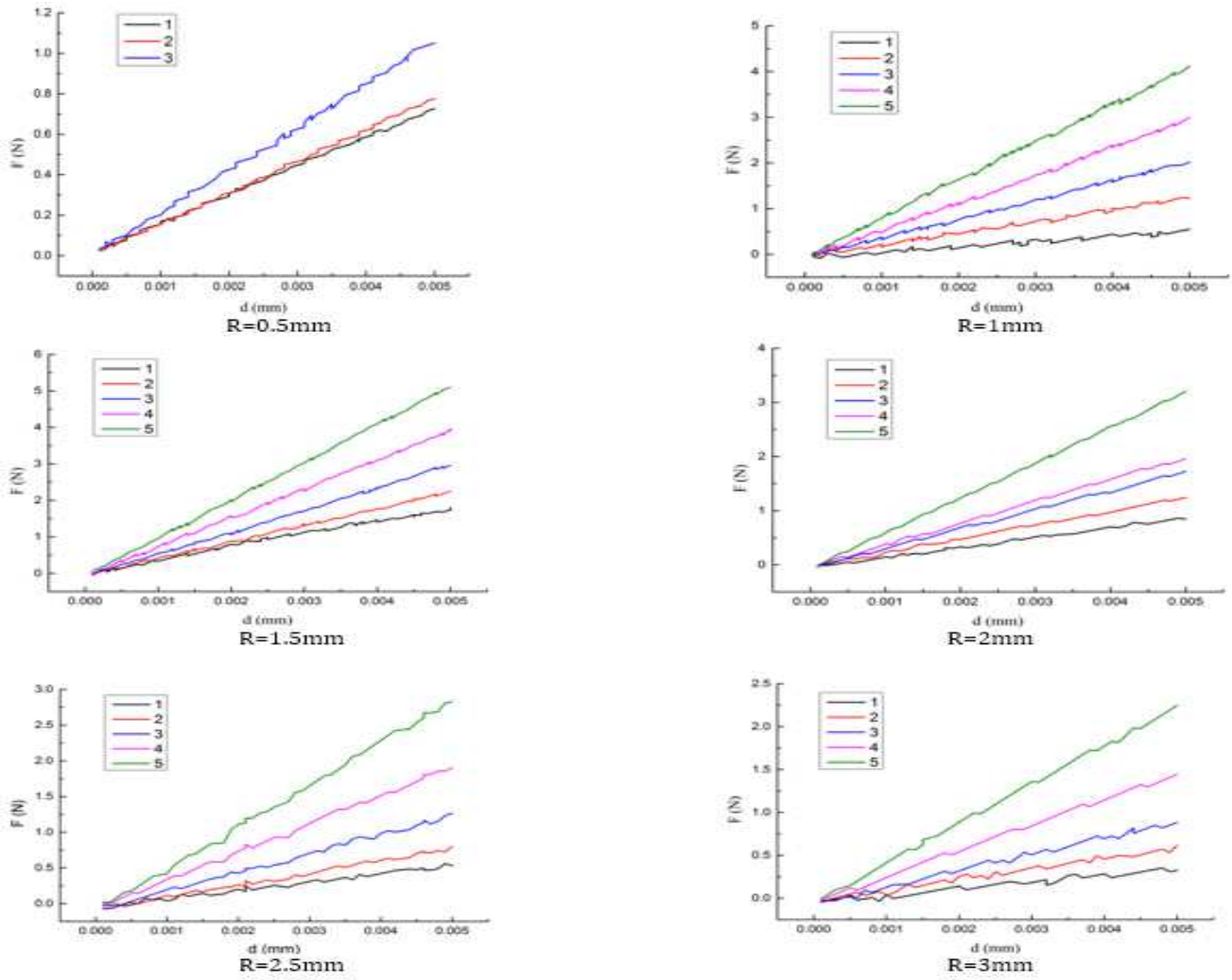

Figure 5. Force-displacement test results

Simulation

As seen in Figure 6, the finite element model of one rubber bush is established in the Abuqus. The rubber bush, placed in a closed cavity formed between the inner and outer metal sleeves, in addition to being constrained radially, is also subject to axial constrain. The axial pre-compression of the rubber bush can be changed by adjusting *s.*

As the rubber bush is assumed to be incompressible, the Poisson's ratio is approximately equal to 0.5. Therefore, the bulk modulus of rubber $k=E/\mathrm{d}(1\text{-}2v)$ tends to be infinite, and the volume strain approaches infinitesimal. In order to compare with the experiment results, six different types of rubber bushes are designed. The cross-sectional shape is shown in Figure 7.

Due to the volume locking phenomenon, the finite element mesh will exhibit excessively rigid behavior, resulting in pseudo-stress in the calculation, which will cause the calculation not to converge, and the higher the material is constrained, the worse this kind of volume locking is. By reducing the integration point in an element, the volume constraints can be released, at the same time by using the hybrid element, the volume locking can be controlled effectively.

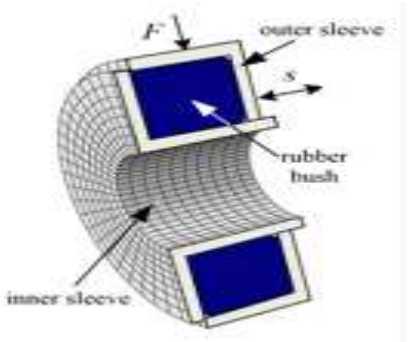

Figure 6. Finite element model of rubber bush inside dynamic vibration absorber

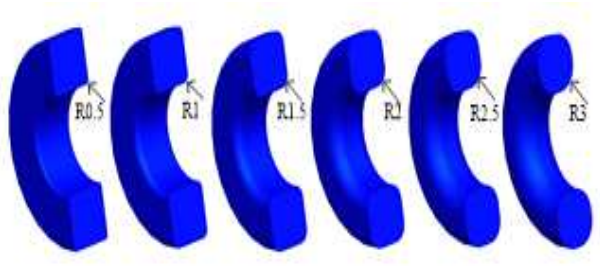

Figure 7. Rubber bushes of different chamfering sizes

According to the friction angle experiment, the dynamic friction coefficient of the metal and rubber is 0.63. By using reduced-integration hybridization elements, a total of 25636 elements are obtained. By loading the out sleeve and fix the inner sleeve, the radial displacement of the rubber bush can be obtained. Figure 8 shows the radial stiffness value of rubber bushes with different chamfering sizes and axial pre-compressions.

Table 3 shows the comparison of simulation results and experimental results. The percentage differences and average differences are listed in the sixth and seventh columns respectively. It is easy to find that the experimentally obtained radial stiffness values are generally lower than the simulation values. The reason is that, in the simulation the outer sleeve is set as an incompressible rigid body, but in the experiment, the outer sleeve is a compressible metal. Therefore under the same force F, in the experiment, the outer sleeve produced larger displacement, which leads to a lower radial stiffness. In addition, it can also be found that the larger the chamfer size is, the greater the deviation between the experimental value and the simulation value is. The main reason is that when the chamfering size is too large, the rubber bush has more free surfaces. During compression, the contact area between the rubber bush and the sleeves changes greatly, which means more non-linear components can be activated. These non-linear components will be followed by further analysis and research. However, it is interesting to note that even the largest magnitude of the average percentage difference, $\%_{aver}$, is only about 10%, which means the simulation results are reliable and can be used for collecting training samples.

Table 3. Comparison of simulation results and experimental results

No.	R (mm)	S (mm)	K_{sim} (N/mm)	K_{expt} (N/mm)	$\%_{diff}$	$\%_{aver}$
1	0.5	0.01, 0.02, 0.03	73.93, 79.12, 107.78	69.23, 77.50, 105.61	-6.36, 2.05, -2.01	-3.47
2	1	0.026, 0.052, 0.078, 0.104, 0.13	58.43, 130.02, 209.39, 311.56, 427.71	55.23, 122.84, 201.86, 299.65, 412.62	-5.48, -5.52, -3.60, -3.82, -3.53	-4.39
3	1.5	0.06, 0.12, 0.18, 0.24, 0.30	179.68, 224.52, 296.09, 389.68, 510.23	162.23, 213.29, 282.5, 374.41, 498.28	-9.71, -5.00, -4.59, -3.92, -2.34	-5.11
4	2	0.108, 0.216, 0.312, 0.432, 0.540	84.75, 124.28, 172.56, 240.97, 320.59	76.63, 115.66, 164.45, 229.64, 309.99	-9.58, -6.94, -4.70, -4.70, -3.20	-5.82
5	2.5	0.168, 0.336, 0.504, 0.672, 0.840	63.35, 86.75, 135.79, 209.86, 308.54	55.32, 78.26, 124.85, 195.36, 289.98	-12.68, -9.79, 8.06, -6.91, -6.02	-8.69
6	3	0.24, 0.48, 0.72, 0.96, 1.20	37.46, 68.63, 98.26, 155.82, 240.16	32.56, 61.54, 88.22, 144.36, 224.56	-13.08, -10.33, -10.22, -7.35, -6.50,	-9.50

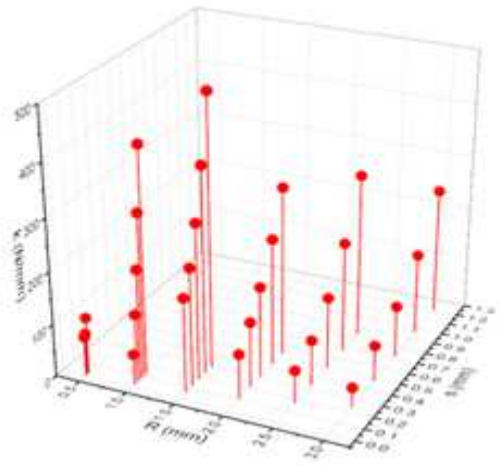

Figure 8. Radial stiffness of rubber bushes

Neural network training

By subdividing the chamfering sizes and axial pre-compressions, 50 training samples are obtained. 70% samples are used for training, 15% samples are used for validation, and the remaining 15% samples are used for testing. Figure 9 shows the regression of the neural network. It is clear to see that the regression of both the training, validation and test samples is up to more than 0.97.

By using the trained neural network, the radial stiffness of the rubber bush can be obtained within a certain range for any chamfering sizes and axial pre-compressions. Make the chamfering size change from 0.5 to 3mm, the axial pre-compressions change from 0 to 1.5mm, the radial stiffness value can be obtained as shown in Figure 10.

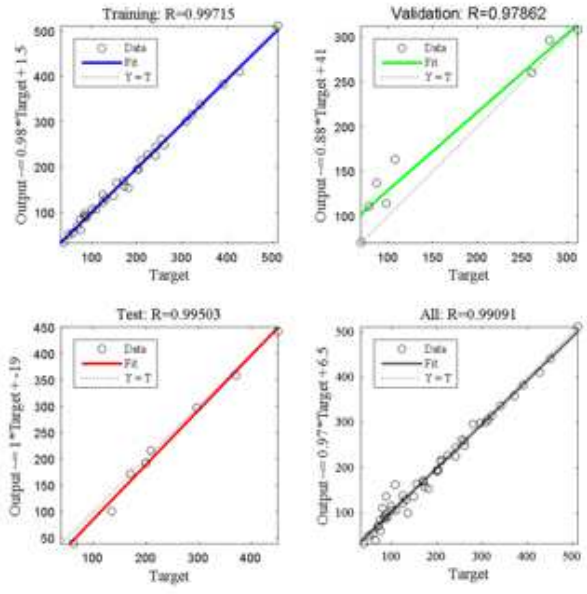

Figure 9. Regression of the neural network

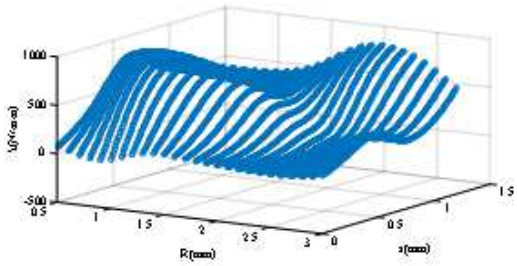

Figure 10. Results of the radial stiffness by using neural network

It can be seen that when the chamfering size is small, with the increase of the axial pre-compression, the rubber bush allows large radial stiffness values. When the chamfering size is large, the radial stiffness does not increase significantly in the early stage, but it does so in the later stage. Therefore, a suitable chamfer size is extremely important for the rubber bush, which can expand the adjustable range of the radial stiffness. When used in dynamic damping boring bar, the dynamic vibration absorber generally performs a small vibration amplitude. Therefore, in order to obtain a larger stiffness adjustable range, a rubber bush having a smaller chamfering size should be selected. According to the training results of the artificial neural network, when the chamfering size is 1.3mm, the axial pre-compression is 0.53mm, and the radial stiffness reaches a maximum of 875.62N/mm. By using the trained artificial neural network, the radial stiffness of the rubber bush for any chamfering sizes and axial pre-compressions can be obtained easily, which provides a great convenience for engineering implementation.

Conclusions

The radial stiffness of the rubber bush has a great influence on the stiffness of dynamic vibration absorber. Analytical formula of radial stiffness under simple boundary conditions has been obtained. But for some more complex cross-section shapes and boundary conditions, it is hard or even impossible to obtain an analytical formula, and thus the artificial neural network method is used to predict the radial stiffness.

A 2-6-1 BP neural network model is established to find the law of radial stiffness of the rubber bush. In order to obtain a good training effect, some specific samples are made, the radial stiffness values of different chamfering sizes and axial pre-compression are obtained through

experiments. Then, the finite element model is established by using Abaqus, and a large number of samples can be obtained through the finite element simulations.

The artificial neural network is trained in the Matlab environment, and the regression of both the training, validation and test samples is up to more than 0.97. By using the trained neural network, the radial stiffness of the rubber bush can be obtained within a certain range for any chamfering sizes and axial pre-compressions. According to the training results of the artificial neural network, when the chamfering size is 1.3mm and the axial pre-compression is 0.53mm, the radial stiffness reaches a maximum of 875.62N/mm.

Acknowledgments

This work is supported by "Basic Research Funds of Southeast University", "the Fundamental Research Funds for the Central Universities", Innovative Plan of Academic Degree Graduate Students in Jiangsu Province, China (Grant No. KYLX16_0186), National Science and Technology Major Project, China (Grant No.2012ZX04002032), and National Science and Technology Major Project, China (Grant No.2013ZX04012032)

References

Adkins JE, Gent AN. Load-deflexion relations of rubber bush mountings. British Journal of Applied Physics 1954; 5(10): 354.

Cheng C, Li S, Wang Y. Performance analysis of high-static-low-dynamic stiffness vibration isolator with time-delayed displacement feedback. Journal of Central South University 2017; 24(10): 2294-305.

Cheng JC, Huang P, Xiong C. Spatial prediction of soil nutrition based on BP neural network. Guangdong Agricultural Sciences 2013; 40(7): 1564-86.

Chuong B, Tung NH, Hung DV. Invited review. Natural rubber nanocomposites. Vietnam Journal of Chemistry 2017; 55(6): 663-78.

Cui X, Gao L, Liu JX. Wind tunnel test study on the influence of railing ventilation rate on the vortex vibration characteristics of the main beam. International Journal of Heat and Technology 2018; 36(1): 65-71.

Ehsani M, Shariatmadari N, Mirhosseini SM. Shear modulus and damping ratio of sand-granulated rubber mixtures. Journal of Central South University 2015; 22(8): 3159-67.

Hill JM. Radical deflections of rubber bush mountings of finite lengths. International Journal of Engineering Science 1975; 13(4): 407-22.

Horton JM, Gover MJC, Tupholme GE. Stiffness of rubber bush mountings subjected to radial loading. Rubber chemistry and technology 2000; 73(2): 253-64.

Horton JM, Tupholme GE. Approximate radial stiffness of rubber bush mountings. Materials & Design 2006; 27(3): 226-29.

Kang Y, Huang CC, Lin CS, Shen PC, Chang YP. Stiffness determination of angular-contact ball bearings by using neural network. Tribology International 2006; 39(6): 461-69.

Li L, Sun B. Optimal parameters selection and engineering implementation of dynamic vibration absorber attached to boring bar//INTER-NOISE and NOISE-CON Congress and Conference Proceedings. Institute of Noise Control Engineering 2016; 253(8): 563-70.

Liu X, Liu Q, Wu S. Analysis of the vibration characteristics and adjustment method of boring bar with a variable stiffness vibration absorber. The International Journal of Advanced Manufacturing Technology 2017; 2017: 1-11.

Liu X, Liu Q, Wu S. Research on the performance of damping boring bar with a variable stiffness dynamic vibration absorber. The International Journal of Advanced Manufacturing Technology 2017; 89(9-12): 2893-906.

Markou AA, Manolis GD. Numerical Solutions for Nonlinear High Damping Rubber Bearing Isolators: Newmark's Method with Netwon-Raphson Iteration Revisited. Journal of Theoretical and Applied Mechanics 2018; 48(1): 46-58.

Maureira N, Llera JDL, Oyarzo C. A nonlinear model for multilayered rubber isolators based on a co-rotational formulation. Engineering Structures 2017; 131: 1-13.

Miguelez MH, Rubio L, Loya JA. Improvement of chatter stability in boring operations with passive vibration absorbers. International Journal of Mechanical Sciences 2010; 52(10): 1376–84.

Qin B, Shao J, Han G. Finite element analyses on radial stiffness of annular rubber in the dynamical vibration absorption boring bar. Machine Design and Research 2008; 24(4): 90-92.

Quintana G, Ciurana J. Chatter in machining processes: A review. International Journal of Machine Tools and Manufacture 2011; 51(5): 363–76.

Rubio L, Loya JA, Miguelez MH. Optimization of passive vibration absorbers to reduce chatter in boring. Mechanical Systems and Signal Processing 2013; 41(1-2): 691-704.

Shuran L, Shujin L. Applying BP neural network model to forecast peak velocity of blasting ground vibration. Procedia Engineering 2011; 26: 257-63.

Siddhpura M, Paurobally R. A review of chatter vibration research in turning. International Journal of Machine Tools and Manufacture 2012; 61: 27–47.

Song W, Cui Z, Yang H. Estimation of Upper Limb Muscle Stiffness Based on Artificial Neural Network. Metrology &Measurement technique 2017; 44(8): 1-3.

Stevenson AC. Some boundary problems of two-dimensional elasticity. Philos. Mag 1943; 34: 766-93.

Yoon JH, Yang IH, Jeong JE. Reliability improvement of a sound quality index for a vehicle HVAC system using a regression and neural network model. Applied Acoustics 2012; 73(11): 1099-103.

Zaoui FZ, Hanifi HA, Abderahman LY, Mustapha MH, Abdelouahed T, Djamel O. Free vibration analysis of functionally graded beams using a higher-order shear deformation theory. Mathematical Modelling of Engineering Problems 2017; 4(1): 7-12.